Talanta 117 (2013) 425–430

Contents lists available at ScienceDirect

Talanta

journal homepage: www.elsevier.com/locate/talanta

Non-aggregation based label free colorimetric sensor for the detection of Cu^{2+} based on catalyzing etching of gold nanorods by dissolve oxygen

Jia-Ming Liu [a,*], Li Jiao [a], Li-Ping Lin [a], Ma-Lin Cui [a], Xin-Xing Wang [a], Li-Hong Zhang [b], Zhi-Yong Zheng [b], Shu-Lian Jiang [c]

[a] Department of Chemistry and Environmental Science, Minnan Normal University, Zhangzhou 363000, PR China
[b] Department of Food and Biological Engineering, Zhangzhou Institute of Technology, Zhangzhou 363000, PR China
[c] Fujian Provincial Bureau of Quality and Technical Supervision, Zhangzhou 363000, PR China

ARTICLE INFO

Article history:
Received 18 June 2013
Received in revised form
30 August 2013
Accepted 3 September 2013
Available online 26 September 2013

Keywords:
Cu^{2+}
Catalytic etching
Gold nanorods
Non-aggregation colorimetric sensor

ABSTRACT

A label-free non-aggregation colorimetric sensor has been designed for the detection of Cu^{2+}, based on Cu^{2+} catalyzing etching of gold nanorods (AuNRs) along longitudinal axis induced by dissolve oxygen in the presence of $S_2O_3^{2-}$, which caused the aspect ratio (length/width) of AuNRs to decrease and the color of the solution to distinctly change. The linear range and the detection limit (LD, calculated by 10 Sb/k, $n=11$) of this sensor were 0.080–4.8 μM Cu^{2+} and 0.22 μM Cu^{2+}, respectively. This sensor has been utilized to detect Cu^{2+} in tap water and human serum samples with the results agreeing well with those of inductively coupled plasma-mass spectroscopy (ICP-MS), showing its remarkable practicality. In order to prove the possibility of catalyzing AuNRs non-aggregation colorimetric sensor for the detection of Cu^{2+}, the morphological structures of AuNRs were characterized by high resolution transmission electron microscopy (HRTEM) and the sensing mechanism of colorimetric sensor for the detection of Cu^{2+} was also discussed.

1. Introduction

Copper ion (Cu^{2+}), besides zinc ion and iron ion, is the most abundant essential transition metal ion in the human body [1]. However, excess doses of copper are extremely poisonous in vivo including cellular toxicity, liver damage, and neurodegenerative diseases [2]. Several diseases, such as Alzheimer's, Parkinson's and Wilson diseases have been proven to be related to the excessive intake of copper [3]. Moreover, Cu^{2+} also incurred serious environmental problems for the wide use in industry. Accordingly, the selective measurement and monitoring of Cu^{2+} in environmental and biological samples are of considerable significance for environment protection and human health.

Up to now, the available methods for Cu^{2+} detection include colorimetry [2–7], electrochemistry [8,9], room temperature phosphorimetry [10], fluorescence sensor [11,12], fluorescence probe [13–15], atomic absorption spectrometry [16,17] and ICP-MS [18].

Unfortunately, among the above methods, some methods require surface modification, some methods need sophisticated and expensive instrumentation, and the procedures used in these methods are time-consuming with partial toxic reagents. Therefore, it should be highly desirable to develop a promising simple and low-cost method tracking for Cu^{2+} in biological, toxicological, and environmental samples to overcome most of those difficulties. Currently, a series of carbon nanotubes [19,20], gold clusters [21], gold and silver nanoparticles [22,23] and other nanomaterials based sensors have been widely used in molecules and ions detection. However, carbon nanotubes need surface modification due to its poor water solubility, silver nanoparticles have poor stability, limiting their practical application. Therefore, searching for simple methods for the determination of trace copper with high stability has been the research focus. Recently, colorimetric sensor has attracted vast attention, because its analyte signal can be directly readout by naked eye, and overcame the traditional colorimetry shortcomings of need organic solvents and dyes. AuNRs exhibit unique optical properties due to its anisotropism, which is mainly attributed to the fact that the location of longitudinal surface plasmon resonance absorption wavelength (LPAW) is highly dependent on the size, shape, surface charge and dielectric condition of AuNRs, while the location of transverse surface plasmon resonance absorption wavelength (TPAW) keeps mostly unchangeable. Accordingly, lots of AuNRs colorimetric sensor have been designed for the detection of dopamine [24], Vitamin C [25], S^{2-} [26], Cr^{6+} [27], Hg^{2+} [28]. The design of more highly sensitive AuNRs colorimetric sensors has become a development trend of the methodology. According to the literature [29], the selectivity and signal amplification effect of catalytic reaction can

* Corresponding author. Tel.: +86 596 2591352; fax: +86 596 2520035.
E-mail addresses: zzsyliujiaming@163.com, zzsyliujiaming@126.com (J.-M. Liu).

0039-9140/$ - see front matter © 2013 Elsevier B.V. All rights reserved.
http://dx.doi.org/10.1016/j.talanta.2013.09.004

improve its selectivity and sensitivity further. Consequently, the possibility of catalytic etching of AuNRs for colorimetric determination of Cu^{2+} was inspected for further improving the selectivity and sensitivity of colorimetric sensor.

Compared with non-catalytic reaction, we found that Cu^{2+} can accelerate the oxidation etching rate of AuNRs by dissolve oxygen with the existence of $S_2O_3^{2-}$ along longitudinal direction due to catalytic effect of Cu^{2+} on dissolved oxygen etching of AuNRs. As a result, the LPAW of AuNRs blue shifts ($\Delta\lambda$) and the color of the solution distinctly changes in this study. Based on the linear relationship between $\Delta\lambda$ and Cu^{2+} content, a novel catalytic non-aggregation colorimetric sensor has been developed for the detection of Cu^{2+}. Compared with aggregation colorimetric probes of AuNRs [2], the innovations of this research were listed as follows:

1. For the detection of Cu^{2+}, the AuNRs non-aggregation sensor was designed based on catalyzing etching of AuNRs by dissolve oxygen showing its new pierce into methodology, while aggregation colorimetric probe was fabricated based on cysteine-modified AuNRs.
2. The sensitivity of AuNRs non-aggregation sensor (LD: 0.22 μM Cu^{2+}) was 5.1 times higher than that (LD: 1.13 μM Cu^{2+}) of aggregation colorimetric probe [2].
3. The non-aggregation AuNRs sensor has the advantage of easy operation without modification, while aggregation AuNRs colorimetric probe requires cysteine-modification. The colorimetric sensor was suitable for the determination of Cu^{2+} in human serum, which provided a new clinical therapy technique for the pregnancy prediction of woman.
4. The signal amplification effect of catalytic reaction can improve the sensitivity of non-aggregation AuNRs sensor, while further improvement of the sensitivity of aggregation colorimetric probe has not been reported.
5. The cross-linking agent with at least two binding sites for the connection with AuNRs is needed during the synthesis process for the construction of aggregation AuNRs colorimetric probe, which limited the applicability of the probe, while the non-aggregation colorimetric sensors of AuNRs obviate the surface modification, making it a promising technique in analysis.

2. Experimental

2.1. Instrumentation and chemicals

Absorption spectra were scanned using a Shimadzu UV-2550 spectrophotometer with one pair of 10-mm quartz cells at room temperature. ICP-MS was performed with ICP-MS instrument (Agilent 7500, USA). The morphological structures of AuNRs were obtained by HRTEM (JEM-2100, Japan Electron Optics Laboratory Co., Ltd) at 200 kV.

$HAuCl_4 \cdot 3H_2O$ (> 99%), $AgNO_3$ (> 99%), $NaBH_4$ (99%), vitamin C (> 99%), hexadecyl trimethyl ammonium bromide (CTAB, 99%), $Na_2S_2O_3$ (> 99%), Cu^{2+} standard solution (GSB G 62024-90(2902), China National Analysis and Testing Centre for Iron and Steel), and all other fundamental reagents (analytical-reagent grade) were purchased from Sinopharm Chemical Reagent Co., Ltd. (Shanghai, China) without further purification. Deionized water and distilled water (18.2 MΩ) were used in all the experiments.

2.2. Synthesis of AuNRs

AuNRs were synthesized according to the silver ion-assisted seed-mediated method reported by Ye et al. [30]. First, 5.00 mL of 0.020 mM $HAuCl_4$ were added to 5.00 mL of 0.20 M CTAB in a 25-mL beaker and stirred. Second, 0.60 mL of 0.010 M $NaBH_4$ (ice-cold) was added and vigorously stirring for 2 min. Finally, the solution was kept in a water bath at 30 °C for 1 h and then used as seed solution.

To prepare AuNRs growth solution, 3.60 g CTAB and 0.32 g Vitamin C were weighed and dissolved with 100 mL water in a 250 mL flask. Next, 2.40 mL of 4.0 mM $AgNO_3$ solution was added and kept undisturbed for 15 min after cooling the solution to 30 °C. Thereafter, 0.50 mL of 0.10 M Vitamin C was added followed by vigorous stirring for 15 min after 100 mL of 1.0 mM $HAuCl_4$ added and then the growth solution was obtained. 0.32 mL seed solution was taken out and added to the growth solution with vigorously stirring for 30 s. Then the solution was aged at 30 °C for 12 h to ensure the full growth of AuNRs for use.

2.3. Experimental method

To a 10.0 mL colorimeter tube, 1.00 mL AuNRs, 1.00 mL of 10^{-3} M $Na_2S_2O_3$, 1.00 mL of 1.0 M NH_4Cl and 1.00 mL of different concentrations of Cu^{2+} were added, then the solution was diluted to 10.0 mL with water. After homogeneously mixed, the mixture solution was incubated at 55 °C water bath for 25 min and then cooled down with running water for 5 min to stop the reaction completely. At the same time, the reagent blank experiment was also carried out. Their absorption spectra were scanned and the LPAW of blank solution (λ_0) and test solution (λ) were recorded correspondingly. Then, the blue shift $\Delta\lambda$ ($=\lambda_0-\lambda$) was calculated.

3. Results and discussion

3.1. Sensing mechanism

In order to demonstrate the sensing mechanism of the response of non-aggregation colorimetric sensor to Cu^{2+}, the UV–vis spectra of the AuNRs–$S_2O_3^{2-}$–Cu^{2+} system were monitored (Fig. 1). Seen from Fig. 1 and Table 1, the prepared AuNRs exhibit two surface plasmon resonance absorption peaks located at 719.0 nm and 520.0 nm, corresponding to LPAW and TPAW, respectively, agree with the optical property of AuNRs [30], indicating the synthesized product is AuNRs.

It was found that the LPAW of AuNRs red shifted for 16.0 nm and corresponding absorbance decreased ($\Delta A=0.108$) in NH_4Cl medium in the presence of $S_2O_3^{2-}$. The reason might be that a part of Au in AuNRs was oxidized by dissolved oxygen to Au(I), which would coordinate with $S_2O_3^{2-}$ to form $Au(S_2O_3)_2^{3-}$, and then Au $(S_2O_3)_2^{3-}$ covered on the surface of AuNRs (Scheme 1) [31], caused

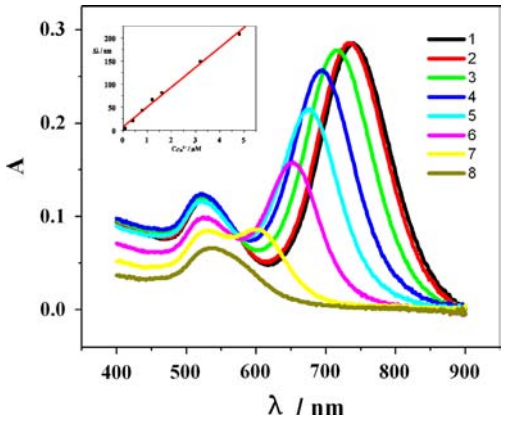

Fig. 1. Vis-absorption spectra of AuNRs–$S_2O_3^{2-}$–Cu^{2+} system (when the contents of Cu^{2+} were 0.80, 4.0, 8.0, 12.0, 16.0, 32.0 and 48.0 (μM), the $\Delta\lambda$ were 4.0, 17.0, 39.0, 62.0, 77.0, 145.0 and 204.0 (nm), the corresponding RSD (%, $n=6$) were 4.7, 4.3, 3.9, 3.4, 3.1, 2.8 and 2.3, respectively).

the absorbance of the AuNRs to decrease. Meanwhile, a small quantity of $S_2O_3^{2-}$ was oxidized to S by dissolved oxygen, and then S reacted with AuNRs to form worm-like Au_2S-Au core–shell structure in the weakly acidic system (Fig. 2b) [32], which caused the aspect ratio of AuNRs to increase, LPAW to red shift and the absorbance of system to decrease further due to the extinction coefficient of Au_2S was lower than that of AuNRs [33].

When 0.80 μM Cu^{2+} was added to the AuNRs–$S_2O_3^{2-}$ system, LPAW of AuNRs blue shifted from 735 nm to 731 nm ($\Delta\lambda$=4.0 nm) followed along with a decrease of absorbance (Fig. 1, curve 3). More interestingly, the increasing of Cu^{2+} concentration caused the $\Delta\lambda$ to gradually enhance and the color of the solution to distinctly change (Fig. 3). This phenomenon could be interpreted that Cu^{2+} has a great catalytic effect on the etching of AuNRs induced by dissolved oxygen in the presence of $S_2O_3^{2-}$ along the longitudinal axis due to the shielding effect of the CTAB on the transverse axis of AuNRs [34]. As a result, Au could react with Cu^{2+} to form Au(I) and Cu^{+}, which would coordinate with $S_2O_3^{3-}$ to form Au $(S_2O_3)_2^{3-}$ and Cu$(S_2O_3)_3^{5-}$, respectively. At the same time, Cu$(S_2O_3)_3^{5-}$ was oxidized to Cu^{2+} by dissolved oxygen (Scheme 2) [35], showing the strong catalytic effect of Cu^{2+} on etching of AuNRs by dissolved oxygen. Meanwhile, the concentration of Cu^{2+} was linear to the $\Delta\lambda$ of the system, which laid the theoretic foundation for the detection of Cu^{2+} using AuNRs non-aggregation colorimetric sensor.

Representative HRTEM images (Fig. 2a) revealed that the length and width of the initial AuNRs were about 50 nm and 12 nm, respectively. When $S_2O_3^{2-}$ and NH_4Cl added, the length of AuNRs kept unchanged and was unevenly distributed while effective aspect ratio of AuNRs increased (Fig. 2b), which was attributed to the formation of worm-like Au_2S-Au core–shell structure. However, the length of AuNRs sharply shortened to ~20 nm while the width kept unchanged due to Cu^{2+} has a greatly catalytic effect on the etching of AuNRs induced by dissolved oxygen when 48 μM Cu^{2+} was added (Fig. 2c). Meanwhile, the morphological characterization changes of AuNRs act powerful demonstration of the aforementioned sensing mechanism of catalyzing AuNRs colorimetric sensor for the detection of Cu^{2+}.

Table 1
The maximum absorption wavelength and the corresponding absorbance of vis-absorption spectra of AuNRs–$S_2O_3^{2-}$–Cu^{2+} system.

	λ_{LPAW}	$\Delta\lambda_{LPAW}$	A_{LPAW}	λ_{TPAW}	A_{TPAW}
1. 1.00 mL AuNRs	719		0.394	520	0.140
2. 1+1.00 mL $S_2O_3^{2-}$	735		0.286	527	0.118
3. 2+0.80 μM Cu^{2+}	731	4	0.279	523	0.118
4. 2+4.0 μM Cu^{2+}	718	17	0.278	521	0.120
5. 2+8.0 μM Cu^{2+}	696	39	0.257	521	0.124
6. 2+12.0 μM Cu^{2+}	673	62	0.215	520	0.116
7. 2+16.0 μM Cu^{2+}	658	77	0.152	520	0.115
8. 2+32.0 μM Cu^{2+}	590	145	0.087	534	0.079
9. 2+48.0 μM Cu^{2+}		204		531	0.064

$$2\,Au + S_2O_3^{2-} + H_2O + 1/2\,O_2 \longrightarrow 2Au(S_2O_3)_2^{3-} + 2\,OH^-$$

Scheme 1. Reaction of the etching of AuNRs by dissolved oxygen in the presence of $S_2O_3^{2-}$.

3.2. Optimization of experimental conditions

For the system containing 1.2 μM Cu^{2+}, the effects of the reagent dosage and concentration, reaction temperature and time on the $\Delta\lambda$ of the system were explored in a univariate approach.

3.2.1. Effect of reagent dosage and concentration

The effects of AuNRs dosage and $S_2O_3^{2-}$ concentration on the $\Delta\lambda$ of the system were examined for obtaining a wide linear range and high sensitivity. As shown in Fig. 4a, the catalytic etching effect of Cu^{2+} on AuNRs and the $\Delta\lambda$ of the system decreased with the increasing of AuNRs dosage. As shown in Fig. 4a, when lowering dosage of the AuNRs, the catalytic effect of Cu^{2+} on the etching of AuNRs by dissolved oxygen increased and the $\Delta\lambda$ of the system accordingly enhanced, with a favorable sensitivity but narrowed linear range compared with high dosage of AuNRs. In contrast, higher dosage expanded the linear range but limited sensitivity. In consideration of both measurement range and sensitivity, 1.00 mL of AuNRs was chosen for the future studies.

As shown in Fig. 4b, the $\Delta\lambda$ of the system reached the maximum when the concentration of $S_2O_3^{2-}$ was 1.0×10^{-3} M; however, the $\Delta\lambda$ of the system decreased when the concentration of $S_2O_3^{2-}$ exceeded 1.0×10^{-3} M. The reason might be that the formation of Au_2S on the surface of AuNRs increased with the

Fig. 3. Color responses when AuNRs react with Cu^{2+} of various concentrations.

$$Au + 5S_2O_3^{2-} + Cu^{2+} \longrightarrow Au(S_2O_3)_2^{3-} + Cu(S_2O_3)_3^{5-}$$
$$O_2$$

Scheme 2. Catalytic effect of Cu^{2+} on etching of AuNRs by dissolved oxygen.

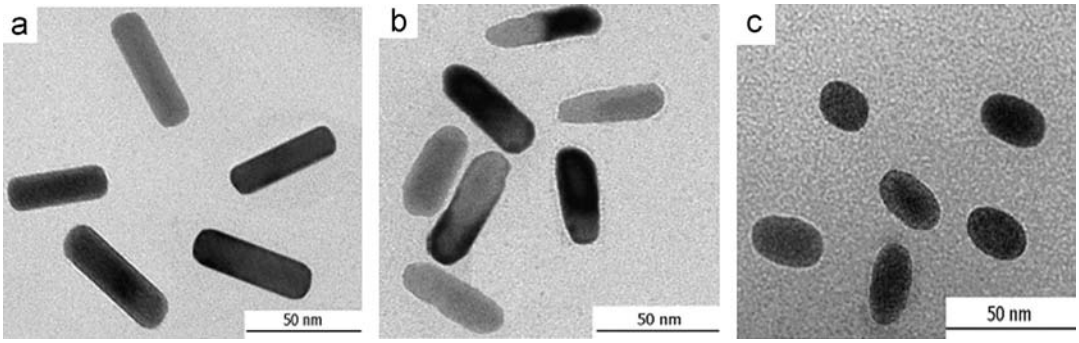

Fig. 2. HRTEM images of (a) AuNRs, (b) AuNRs–$S_2O_3^{2-}$ and (c) AuNRs–$Na_2S_2O_3$–Cu^{2+}.

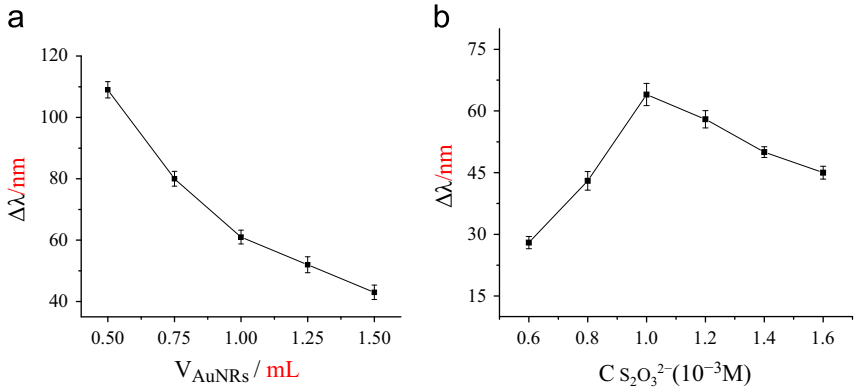

Fig. 4. Effect of AuNRs dosage (a) and $S_2O_3^{2-}$ concentration (b) on the $\Delta\lambda$ of the system.

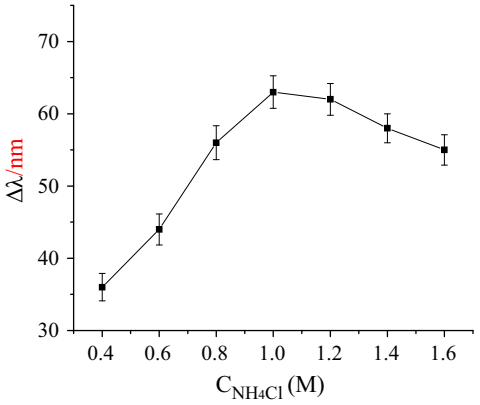

Fig. 5. Effect of the NH_4Cl concentration on the $\Delta\lambda$ of the system.

increasing of the concentration of $S_2O_3^{2-}$, limiting the etching of AuNRs. Therefore, 1.0×10^{-3} M $S_2O_3^{2-}$ was chosen as the optimum concentration.

In this study, the influence of the concentration of NH_4Cl on the $\Delta\lambda$ of the system was investigated using NH_4Cl as the medium due to Cl^- in NH_4Cl would coordinate with Au(I) to form $AuCl_4^-$ causing the electric potential of Au(I)/Au(0) decreasing (the standard electron potential of $AuCl_4^-$/Au(0) is 1.15 V, which is lower than that of 1.83 V of Au(I)/Au(0) [36]). As shown in Fig. 5, the $\Delta\lambda$ of the system reached the maximum when the concentration of NH_4Cl was 1.0 M; however, the $\Delta\lambda$ of the system decreased when the concentration of NH_4Cl exceeded 1.0 M. This was attributed to the fact that the electric potential of Au(I)/Au (0) gradually decreased with the increasing the concentration of NH_4Cl, accelerating the etching of AuNRs. Thus, 1.0 M NH_4Cl was chosen for the following studies.

3.2.2. Effect of reaction temperature and time

In order to avoid thermal reshaping of AuNRs, the temperature effect on the etching reaction was investigated only in the range of 25–60 °C. As shown in Fig. 6, the selective etching ($\Delta\lambda$) depends on both reaction temperature and time. At a fixed reaction time of 25 min, the $\Delta\lambda$ of the system increase with the increasing of temperature and reached the maximum at 55 °C (Fig. 6a). The reason might be that the catalytic etching rate of AuNRs gradually was promoted with the increasing temperature and reached the maximum at 55 °C. The reaction temperature was adjusted to 55 °C, the selective etching by 1.2 μM Cu^{2+} completed in 25 min (Fig. 6b) and the system remained stable. This was attributed to the signal amplification effect of Cu^{2+} catalytic etching of AuNRs by dissolved oxygen which reached the maximum after 25 min. Taking those factors into account, the reaction was carried out at 55 °C for 25 min.

3.2.3. Stability of the system

Under the optimum conditions, for the system containing 1.2 μM Cu^{2+}, when the system stood for 5, 10, 15, 20, 25 and 30 (min) after being cooled by flowing water for 5 min, the $\Delta\lambda$ of the system were 61.0, 62.0, 62.0, 63.0, 64.0 and 63.0 (nm), and the corresponding RSDs were 2.6, 2.8, 3.3, 3.2, 2.9 and 2.5 (%), respectively. Results show that the $\Delta\lambda$ of the system remained unchanged in 10–30 min showing good stability of the system.

3.3. Working curve, linear range and sensitivity

The linear range, the corresponding linear regression equations of the working curve, correlation coefficient (r), RSD% (0.0800 and 4.8 μM Cu^{2+} were separately determined in parallel for 7 times), detection limit (DL, calculated by 3Sb/k which referred to the quotient between three of the blank reagent's standard deviation (Sb=0.91, n=11) and the slope of the working curve) and LD (calculated by 10Sb/k) of this colorimetric sensor were compared with those of Ref. [2] under the optimum conditions, respectively. Results are listed in Table 2.

As shown in Table 2, though the linear range of this proposed non-aggregation AuNRs colorimetric sensor was narrower than that of cross-linking colorimetric probe, but AuNRs colorimetric sensor possessed higher sensitivity. This was attributed to the signal amplification effect of Cu^{2+} catalytic etching of AuNRs. Moreover, compared with cross-linking colorimetric probe [2], this sensor without surface modification operated easily (Table 3) and was more suitable for analysis of low content Cu^{2+} in real samples.

3.4. Selectivity

For the system containing 1.2 μM Cu^{2+}, the selectivity of the sensor was evaluated by testing the response of the sensor to the co-existing ions in tap water samples under optimum conditions. When the relative error (Er) exceeded ±5%, the ion was considered as an interfering agent. Results found that K^+, Ca^{2+}, Na^+, Mg^{2+}, Al^{3+}, Zn^{2+}, Ni^{2+}, Ba^{2+}, Co^{2+}, Cd^{2+}, Cr^{3+}, Pb^{2+}, Hg^{2+} (0.2 mM), amylum (0.83 mM), sucrose (0.64 mM), glucose (0.625 mM), citric acid (0.54 mM) and tartaric acid (0.48 mM) have no obvious response to the sensor. The Fe^{3+} (20 μM) had weak interference and the influence of Fe^{3+} could be completely eliminated by adding H_3PO_4. Fe^{2+} (50 μM), Mn^{2+} (40 μM) and Sn^{2+} (30 μM) had interference because they can react with dissolve oxygen and they could be completely eliminated by adding mixed solution of 0.50 mL of 5% NaF, 1.00 mL of 8%

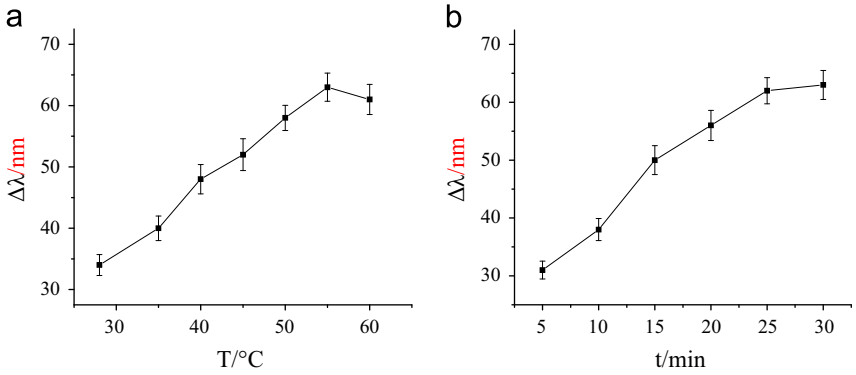

Fig. 6. Effect of reaction temperature (a) and time (b) on the $\Delta\lambda$ of the system.

Table 2
Comparison of analysis parameters.

Method	Linear range (μM)	Regression equation ($n=7$)	r	RSD (%)	DL (μM)	LD (μM)
Non-aggregation AuNRs colorimetric sensor	0.080–4.8	$\Delta\lambda=4.869+42.54$ [Cu^{2+}] (μM)	0.9978	2.7	0.066	0.22
Cross-linking colorimetric probe [2]	1–100	$\Delta R=0.021+0.016C$ (μM)	0.9845	1.8	0.34	1.13

Table 3
Comparison of analysis methods.

Method	Mechanism for the detection of Cu^{2+}	Modification	AuNRs status	Method of improving sensitivity	Sensitivity
Non-aggregation AuNRs colorimetric sensor	The colorimetric detection of Cu^{2+} based on catalyzing etching of gold nanorods by dissolve oxygen	Wthout surface modification	Non-aggregation AuNRs	Method of signal amplification effect	High
Cross-linking colorimetric probe [2]	The colorimetric detection of Cu^{2+} using cysteine – modified AuNRs	Mdified AuNRs by cysteine	Agregation AuNRs	It not been reported	Low

Table 4
Determination of Cu^{2+} in table tap water samples (the addition of Cu^{2+} is 0.10 μM).

This non-aggregation AuNRs colorimetric sensor ($n=6$)							ICP-MS ($n=6$)			Statistical analysis		
Samples	$\overline{X}_1$ (μM)	Found (μM)	Recovery (%)	RSD (%)	S_1	Er	$\overline{X}_2$ (μM)	RSD (%)	S_2	F	$\overline{S}$	t
A	0.96	0.102	102	2.5	0.024	−2.0	0.98	2.6	0.025	1.08	0.0245	1.41
B	1.18	0.097	97	2.2	0.026	2.6	1.15	1.8	0.021	1.53	0.0235	2.21
C	1.05	0.104	104	2.2	0.023	−1.0	1.06	2.7	0.029	1.74	0.026	0.67

hydroxylamine hydrochloride and 0.20 mL of 3% trolamine. Ag^+ (100 μM) can react with $S_2O_3^{2-}$ while it could be completely eliminated by adding 1.50 mL of 2% $NH_3\cdot H_2O$ solution. The results prove that the sensor has a good selectivity.

3.5. Real sample analysis

In order to test the practicality of this method, the sensor was applied to determine the content of Cu^{2+} in real samples. Three kinds of tap water samples (A, B and C) were taken to detect the Cu^{2+} content according to the above experimental method. Meanwhile, the standard addition recovery experiment was carried out. The results were compared with those obtained by ICP-MS and listed in Table 4.

Seen from Table 4, when the $P=0.95$, $f=n_1+n_2-2=10$, the corresponding $F_{0.95,\ 10}=5.05$ was larger than 1.08, 1.53 and 1.74 toward the samples of A, B and C, indicating that there was no significant difference between S_1 and S_2; and the $t_{0.95,\ 10}=2.23$ was larger than 1.41, 2.21 and 0.67, indicating that there was no significant difference between $\overline{X}_1$ and $\overline{X}_2$. Furthermore, the Er of this method was less than $\pm$5% and the recovery was in the range of 97.0–102%, showing a good accuracy of this sensor. Therefore, this sensor was suitable to the detection of Cu^{2+} in tap water samples.

In order to test further the practicality of this method, the sensor was applied to determine the content of Cu^{2+} in analyzing certified reference materials and human serum. Conventionally, each 2.00 mL blood of fasting vein was respectively taken from not pregnant woman, normal pregnant woman and normal man. The blood samples were stood for 4 h at room temperature, centrifugalized at the speed of 3000 r min^{-1} for 20 min, the serum was transferred into a colorimetric tube and kept at −20 °C for use. Two milliliter of the human serum was diluted to 10 mL for the determination of Cu^{2+}. Meanwhile, a standard addition recovery experiment was also conducted. Results were compared with those obtained by detection kit of Cu^{2+} in human serum and listed in Table 5.

Table 5
Analytical results of Cu^{2+} in human serum ($n=6$).

Item	Not pregnant woman ($n=50$)	Normal pregnant woman ($n=25$)	Normal man ($n=50$)
Age (year)	20–40	23–40	23–55
Found of non-aggregation AuNRs colorimetric sensor (μM)	7.2–27.5	21.3–40.8	10.8–21.9
Average found ($\overline{X}$, μM)	17.2	34.8	15.6
RSD (%)	4.2	3.6	2.5
Cu^{2+} in human serum by detection kit (μM)	7.6–28.1	21.8–40.6	10.5–20.2
Reference value of Cu^{2+} in analyzing certified reference human serum (μM)	13.3–24.2	25.3–41. 0	11.0–22.0

Table 5 shows that this method could be applied to determine Cu^{2+} in human serum and the results were consistent with those of detection kit. Moreover, according to reference value of Cu^{2+} in analyzing certified reference human serum, the content of Cu^{2+} in serum of not pregnant woman and pregnant woman are within 13.3–24.2 μM and 25.3–41.0 μM. If the content of Cu^{2+} in human serum was in the range of 7.2–27.5 μM, they might be not pregnant woman; when the content of Cu^{2+} in human serum was in the range of 21.3–40.8 μM, they might be pregnant woman. Results show that the non-aggregation AuNRs colorimetric sensor was suitable for the determination of Cu^{2+} in human serum, which reflected a brighter clinical application prospect, and also provided a new clinical therapy technique for the pregnant prediction of woman.

4. Conclusions

A non-aggregation colorimetric sensor for the determination of Cu^{2+} has been designed based on catalyzing etching of AuNRs by dissolve oxygen, and this sensor without surface modification has many merits such as operation is simple, accurate, sensitivite and selectivite, exhibiting the broad application prospect in water and human serum analysis. This study not only provided new ways for the application of catalytic reaction, but also advanced the interpenetration among catalytic kinetic, nanoscale science and trace analysis of inorganic ions. This research also shows that combining the catalytic kinetic analysis method with colorimetric analysis technology is the future research direction of AuNRs non-aggregation colorimetric sensor.

Acknowledgments

This work was supported by the Fujian Province Natural Science Foundation (Grant nos. 2010J01053 and JK2010035), the Fujian Province Education Committee (JA11164, JA11311, JA10203 and JA10277), the Fujian provincial bureau of quality and technical supervison (FJQI 2011006) and the Scientific Research Program of Zhangzhou Institute of Technology Foundation (Grant nos. ZZY 1106 and ZZY 1014). At the same time, we are very grateful for the precious advices raised by the anonymous reviewers.

References

[1] D.W. Domaille, E.L. Que, C.J. Chang, Nat. Chem. Biol. 4 (2008) 168–175.
[2] J.M. Liu, H.F. Wang, X.P. Yan, Analyst 136 (2011) 3904–3910.
[3] Y.J. Song, K.G. Qu, C. Xu, J.S. Ren, X.G. Qu, Chem. Commun. 46 (2010) 6572–6574.
[4] Y. Zhou, S.X. Wang, K. Zhang, X.Y. Jiang, Angew. Chem. Int. Ed. 47 (2008) 1–4.
[5] B.C. Yin, B.C. Ye, W.H. Tan, H. Wang, C.C. Xie, J. Am. Chem. Soc. 131 (2009) 14624–14625.
[6] T. Gunnlaugsson, J.P. Leonard, N.S. Murray, Org. Lett. 6 (2004) 1557–1560.
[7] Y. Zhou, H. Zhao, Y.J. He, N. Ding, Q. Cao, Colloids Surfaces A 391 (2011) 179–183.
[8] P. Salaun, C.M.G. van den Berg, Anal. Chem. 78 (2006) 5052–5060.
[9] B.K. Jena, C.R. Raj, Anal. Chem. 80 (2008) 4836–4844.
[10] Z.M Li, J.M Liu, Z.B. Liu, Q.Y. Liu, X. Lin, F.M. Li, M.L Yang, G.H. Zhu, X.M. Huang, Anal. Chim. Acta 589 (2007) 44–50.
[11] Z.C. Wen, R. Yang, H. He, Y.B. Jiang, Chem. Commun. (2006) 106–108.
[12] X. Ma, Z.W. Tan, G.H. Wei, D.B. Wei, Y.G. Du, Analyst 137 (2012) 1436–1439.
[13] C.V. Durgadas, C.P. Sharma, K. Sreenivasan, Analyst 136 (2011) 933–940.
[14] J.M. Liu, L.P. Lin, X.X Wang, S.Q. Lin, W.L. Cai, L.H. Zhang, Z.Y. Zheng, Analyst 137 (2012) 2637–2642.
[15] Y.Q. Dong, R.X. Wang, G.L. Li, C.Q. Chen, Y.W. Chi, G.N. Chen, Anal. Chem. 84 (2012) 6220–6224.
[16] M.S. Chan, S.D. Huang, Talanta 51 (2000) 373–380.
[17] İ. Durukan, Ç.A. Şahin, S. Bektaş, Microchem. J. 98 (2011) 215–219.
[18] J.F. Wu, E.A Boyle, Anal. Chem. 69 (1997) 2464–2470.
[19] H. Beitollahi, H. Karimi-Maleh, H. Khabazzadeh, Anal. Chem. 80 (2008) 9848–9851.
[20] H. Beitollahi, J.B. Raoof, H. Karimi-Maleh, R. Hosseinzadeh, J. Solid State Electrochem. 16 (2012) 1701–1707.
[21] M.L. Cui, J.M. Liu, X.X. Wang, L.P. Lin, L. Jiao, L.H. Zhang, Z.Y. Zheng, S.Q. Lin, Analyst 137 (2012) 5346–5351.
[22] M. Rycenga, C.M. Cobley, J. Zeng, W.Y. Li, C.H. Moran, Q. Zhang, D. Qin, Y.N. Xia, Chem. Rev. 111 (2011) 3669–3712.
[23] M.C. Daniel, D. Astruc, Chem. Rev. 104 (2004) 293–346.
[24] J.M. Liu, X.X. Wang, M.L. Cui, L.P. Lin, S.L. Jiang, L. Jiao, L.H. Zhang, Sensors Actuators B Chem. 176 (2013) 97–102.
[25] X.X. Wang, J.M. Liu, S.L. Jiang, L. Jiao, L.P. Lin, M.L. Cui, X.Y. Zhang, L.H. Zhang, Z. Y. Zheng, Sensors Actuators B Chem. 182 (2013) 205–210.
[26] J.M. Liu, X.X. Wang, F.M. Li, L.P. Lin, W.L. Cai, X. Lin, L.H. Zhang, Z.M. Li, S.Q. Lin, Anal. Chem. Acta 708 (2011) 130–133.
[27] F.M. Li, J.M. Liu, X.X. Wang, L.P. Lin, W.L. Cai, Y.N. Zeng, L.H. Zhang, S.Q. Lin, Sensors Actuators B Chem. 155 (2011) 817–822.
[28] M. Rex, F.E. Hernandez, A.D. Campiglia, Anal. Chem. 78 (2006) 445–451.
[29] J.M. Liu, X.J. Cui, L.M. Li, G.M. Fu, S.X. Lin, M.L. Yang, M.Y. Xu, Z.Q. Wu, Spectrochim. Acta Part A 66 (2007) 1194–1198.
[30] X.C. Ye, L.H. Jin, H.R. Caglayan, J. Chen, G.Z. Xing, C. Zheng, V. Doan-Nguyen, Y. J. Kang, N. Engheta, C.R. Kagan, C.B. Murray, Nano 6 (2012) 2804–2817.
[31] Y.Y. Chen, H.T. Chang, Y.C. Shiang, Y.L. Hung, C.K. Chiang, C.C. Huang, Anal. Chem. 81 (2009) 9433–9439.
[32] H.W. Huang, C.C. He, Y.L. Zeng, X.D. Xia, X.Y. Yu, P.G. Yi, Z. Chen, J. Colloid Interface Sci. 322 (2008) 136–142.
[33] J.M. Liu, X.X. Wang, F.M. Li, L.P. Lin, W.L. Cai, X. Lin, L.H. Zhang, Z.M Li, S.Q. Lin, Anal. Chim. Acta 708 (2011) 130–133.
[34] R.X. Zou, X. Guo, J. Yang, D.D. Li, F. Peng, L. Zhang, H.J. Wang, H. Yu, CrystEngComm 11 (2009) 2797–2803.
[35] T.T. Lou, L.X. Chen, Z.P. Chen, Y.Q. Wang, L. Chen, J.H. Li, ACS. Appl. Mater. Interfaces 3 (2011) 4215–4220.
[36] C.K. Tsung, X.S. Kou, Q.H. Shi, J.P. Zhang, M.H. Yeung, J.F. Wang, G.D. Stucky, J. Am. Chem. Soc. 128 (2006) 5352–5353.